Journal of Gerontology: BIOLOGICAL SCIENCES
2005, Vol. 60A, No. 7, 000–000

Early-Senescing Human Skin Fibroblasts Do Not Demonstrate Accelerated Telomere Shortening

Marina Ferenac,[1] Denis Polančec,[2] Miljenko Huzak,[3]
Olivia M. Pereira-Smith,[4] and Ivica Rubelj[1]

[1]Department of Molecular Biology, Ruđer Bošković Institute, Zagreb, Croatia.
[2]PLIVA-Research Institute Ltd., Biology, Flow Cytometry and Cell Sorting Lab, Zagreb, Croatia.
[3]Department of Mathematics, University of Zagreb, Croatia.
[4]Department of Cellular and Structural Biology, Sam and Ann Barshop Center for Longevity and Aging Studies, San Antonio, Texas.

Most normal mammalian cell lines demonstrate limited growth capacity due to the gradual accumulation of senescent cells in the culture. Senescent cells appear initially at a low incidence, but with increasing frequency as the culture accumulates more divisions. Because it has been suggested that senescence is regulated by telomere shortening in human cells, we compared the telomere lengths of the subpopulation of senescent cells, present in presenescent cultures, with those of young cells. Senescent cells were separated from young cycling cells by either bromodeoxyuridine (BrdU) incorporation followed by Hoechst dye and light treatment or DiI staining followed by separation on a high-speed cell sorter. Our results demonstrate that telomeres of early-senescing cells are the same length, and must shorten at the same rate, as cycling sister cells in the culture. Therefore, senescent cells in young mass cultures occur as a result of a stochastic, nontelomere-dependent process that we have described: sudden senescence syndrome.

MOST normal mammalian cell lines demonstrate a common growth pattern during proliferation in vitro. Cultures initially have a period of rapid growth during which the majority of the cells divide vigorously. As the culture accumulates more divisions, the growth potential declines due to the gradual increase in the fraction of nondividing, senescent cells. Eventually, the entire culture enters the terminally nondividing state, referred to as replicative senescence (1,2). Upon growth cessation, senescent cells do not die, but remain viable in the culture, and undergo various morphological and biochemical changes, e.g., cell size enlargement, endogenous senescence-associated senescence-associated β-galactosidase (SA-β-gal) staining at pH 6.0 (3–5), and altered gene expression (6,7). It has been described that senescent cells appear in the culture in a stochastic manner (8), and this can occur within the period of one cell division. For example, in daughter cell experiments, Smith and Whitney (8) demonstrated that the degree of difference in doubling potentials between two cells arising from a single mitotic event can vary from 0 to greater than 8 population doublings (PDs), and even more cell generations (9). This stochastic aspect of cellular aging is an intriguing but not well understood phenomenon. A few models have been proposed suggesting that these and other characteristics of cell senescence have their origins in processes related to the maintenance of telomeres, repetitive sequences at the ends of all eukaryotic chromosomes. These models include abrupt shortening of one or a few telomeres in the cell (10), stochastic uncapping of telomeres (11), or accelerated telomere shortening in a subpopulation of cells (12,13). To examine this, we analyzed telomere length of the early-senescing cell subpopulation present in actively dividing normal human fibroblast cultures. Fractions of nondividing senescent cells were isolated from cycling cultures by either bromodeoxyuridine (BrdU) incorporation followed by Hoechst dye and light treatment or by 1,1′-dioctadecyl-3,3,3′,3′-tetramethylindocarbocyanineperchlorate (DiI) staining and separation on a high-speed flow cytometer–cell sorter. Telomere lengths of the selected populations of young versus senescent cells were then determined.

Experimental Procedures

Cell Lines and Culture Conditions

Normal human foreskin fibroblast (NF) cells were isolated from the upper arm of a 7-year-old female donor at the Neurochemical Laboratory, Department of Chemistry and Biochemistry School of Medicine, University of Zagreb. HCA2 (MJ90) cells were isolated previously from neonatal foreskin in the Pereira-Smith laboratory. Cells were grown in Dulbecco's modified Eagle's medium (DMEM; Sigma, St. Louis, MO), supplemented with 10% fetal bovine serum (FBS) and sodium carbonate at 3.7 mg/ml in 5% CO_2. Under these conditions, the NF and HCA2 cultures consistently and from many, independently thawed frozen stocks undergo 55 and 70 PDs prior to senescence, respectively.

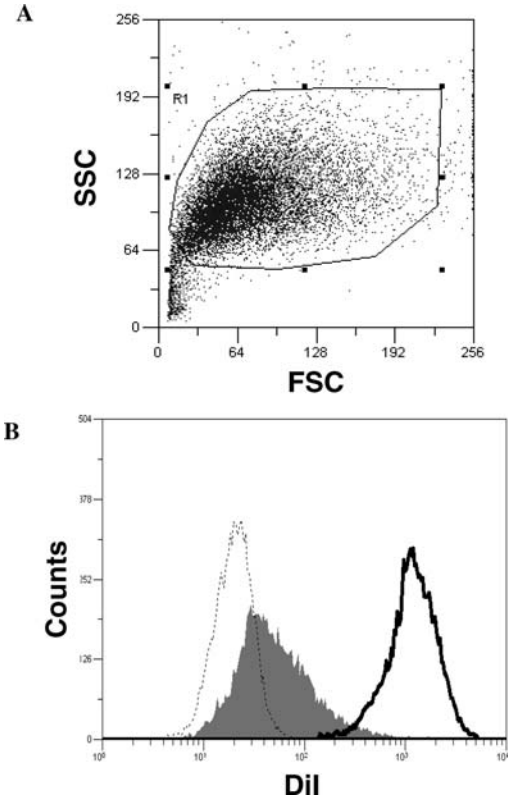

Figure 1. Gating strategy and sorted cells analysis. **A**, Polygonal region was drawn around cells according to their morphological properties on a forward-scatter light (FSC) and/or side-scatter light (SSC) dot plot. Live cells are gated, whereas dead cells and cell debris were excluded from further analysis and sorting. **B,** Overlay histograms of unstained 7-day-old culture control cells (dashed line), 7-day-old control culture cells stained with 1,1′-dioctadecyl-3,3,3′,3′-tetramethylindocarbocyanineperchlorate (DiI) at the day of experiment (thick line), and DiI-stained cells analyzed after 7 days in culture (gray filled). **C,** Sort decisions were made combining live cell gate (A) with region R1 (most divided cells; blue colored gate) for one sort direction and R2 (nondivided cells; red colored gate) for another sort direction. Part of each sorted cell population was cultivated for morphology and senescence-associated-β-galactosidase (SA-β-gal) activity analysis. PC = phase contrast. Dividing fraction demonstrates young phenotype and poor SA-β-gal staining, whereas nondividing fraction demonstrates senescent phenotype and intense SA-β-gal staining. **D,** Clear separation of two cell groups is shown using overlay histogram of analyzed cells from both populations sorted. Sort purity was ≥98% in all sorting experiments performed. Data are representative of three different experiments.

BrdU Selection

NF cells were seeded at approximately 50% confluence (2×10^4 cells/cm^2) in four T75 tissue-culture flasks (75 cm^2; Techno Plastic Products, Trasadingen, Switzerland) containing 20 ml of medium with serum and 20 μM BrdU (Sigma), and were incubated at 37°C under a light-tight aluminum cover. After 1 week, the cells were rinsed with DMEM without serum and refed with DMEM containing 1.6 μM 33258 Hoechst dye. The cultures were incubated in the dark for 2.5 hours and then irradiated from above by cool white fluorescent bulbs as previously described (14,15). This treatment was repeated weekly for up to 4 weeks during which time cell death of cycling cells occurred. When all the dividing cells had been eliminated, as monitored by microscopy, the cells from all four flasks were collected by trypsinization and pooled for DNA isolation and flow cytometric analysis. An aliquot of 5×10^4 cells was seeded into 35 mm tissue culture dishes for SA-β-gal staining.

DiI Labeling and Flow Cytometry

NF or HCA2 cells were trypsinized and stained in suspension for 20 minutes in 5 μM solution of DiI (catalog No. D282, 100 mg; Molecular Probes, Eugene, OR), washed twice, and cultured in the dark. After 5–7 days, cells were trypsinized, washed twice in freshly prepared PBS (Sigma) containing 2% FBS (Sigma) and 0.02% EDTA (Sigma), resuspended in the same buffer at 2.5×10^7/ml, and kept on ice until sorting. Control cells were stained for 20 minutes and placed on ice in the same buffer until sorting. Cells were analyzed and sorted on a MoFlo high-speed cell sorter (DakoCytomation, Glostrup, Denmark) using Summit software (DakoCytomation); a 488 nm Argon-Ion laser tuned on 125 mW of power was used as a source of excitation. Forward-scattered light and side-scattered light were detected with linear signal amplification (Figure 1), whereas DiI-specific fluorescence emission was detected on the FL2 channel using a 570/30 dichroic emission filter and logarithmic signal amplification. Two separate cell populations were sorted simultaneously into 14 ml Falcon tubes coated with 100% FBS and containing 1 ml of FBS. Collected cells were centrifuged, resuspended in culture medium, counted, and used for DNA isolation and SA-β-gal staining.

SA-β-Gal Staining

For senescence-associated SA-β-gal staining, cells were plated into 30 mm tissue-culture dishes. Twenty-four hours later the cells were fixed and stained as described previously (5).

Southern Blot Analysis

Genomic DNA was isolated with a DNeasy Tissue Kit (Qiagen, Valencia, CA) and digested with RsaI/HinfI (Roche, Indianapolis, IN) restriction enzymes. Equal amounts (5 μg) of DNA were loaded on 0.8% agarose gel. DNA was transferred to nitrocellulose membranes (Roche) by capillary transfer, the membrane hybridized with digoxigenin-labeled terminal restriction fragment (TRF) telomere-specific probe detected with CDP-Star (Roche) using X-ray film (Kodak). The TRF telomere digoxigenin-labeled probe was prepared by polymerase chain reaction (PCR). Primers specific for the telomere sequence F: $(CCCTAA)_4$, R: $(TTAGGG)_4$ were amplified by non-template PCR (94°C/1.5 min, 94°C/45 s, 52°C/30 s, 72°C/1 min, 72°C/10 min; 30 cycles).

Densitometry and Telomere Length Analysis

Prior to densitometry, X-ray films were scanned with a UMAX Astra 4000U scanner (UMAX Technologies Inc., Dallas, TX). Densitometry was performed using Image-Master VSD software (Amersham Biosciences, U.K.), Pharmacia Biotech, and data were analyzed using Mathematica 4 (Wolfram Research, Inc., Champaign, IL). Mean

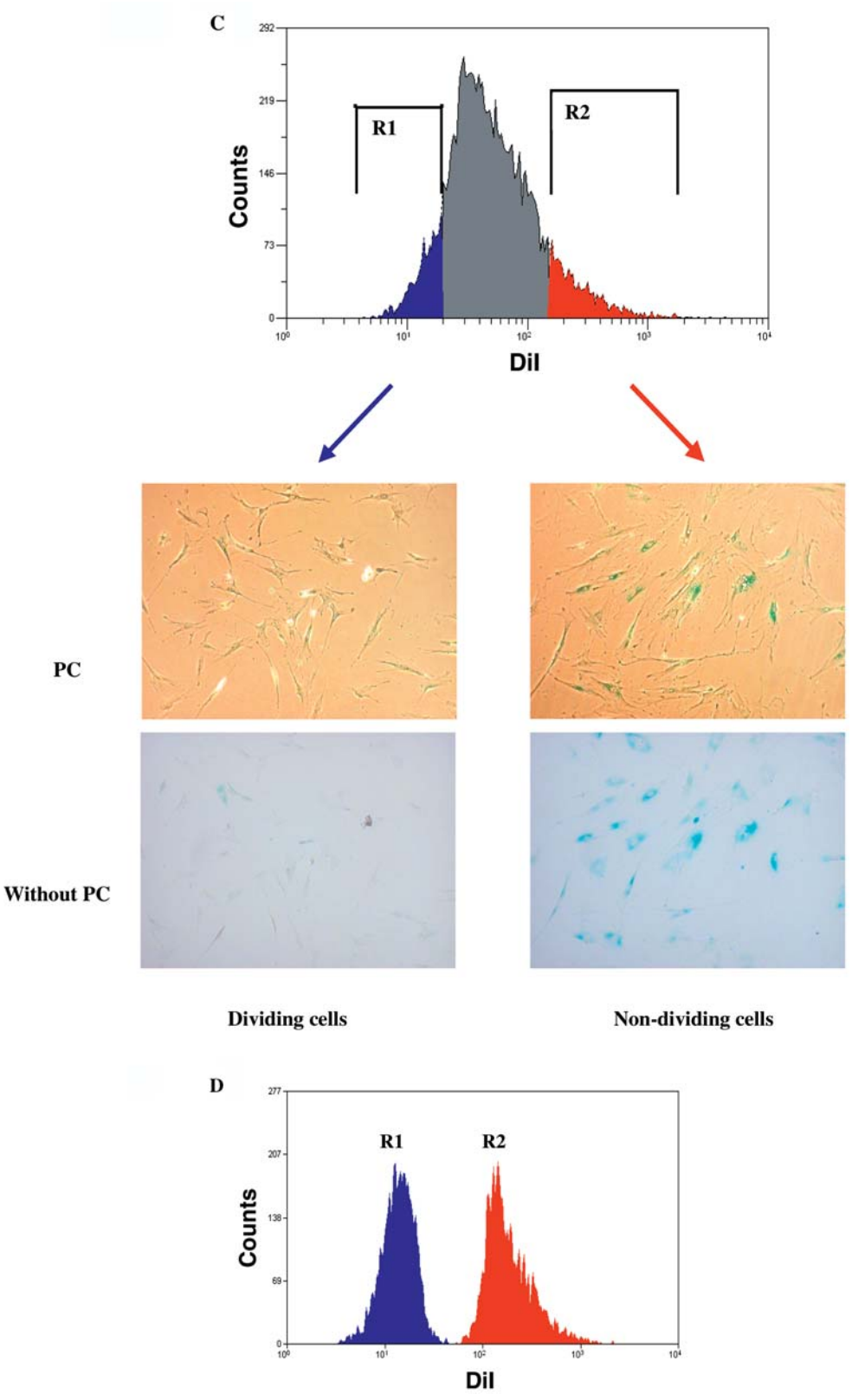

Figure 1. (Continued).

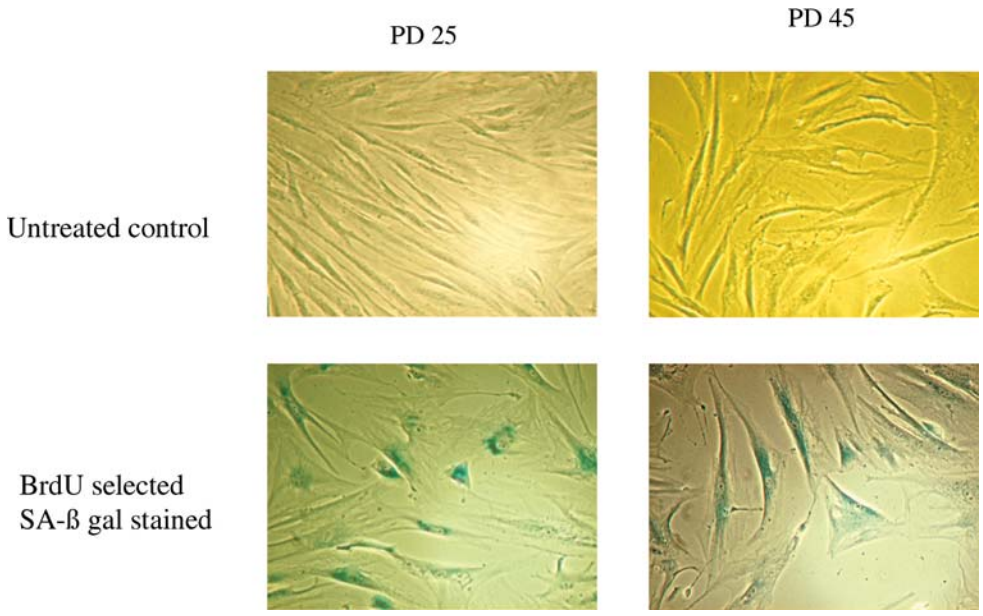

Figure 2. Untreated control cells at population doublings (PDs) 25 (young) and 45 (senescent) and senescence-associated-β-galactosidase (SA-β-gal) activity of their BrdU-selected fractions. Senescent phenotype of bromodeoxyuridine (BrdU)-selected fraction of young culture is clearly visible and resembles its senescent counterpart.

telomere length and standard deviation was determined using the following formulas:
For mean telomere lengths:

$$\mu = \frac{\sum_i f_i \cdot L_i}{\sum_i f_i} = \frac{\sum_i OD_i}{\sum_i \frac{OD_i}{L_i}}$$

For standard deviation:

$$\sigma = \sqrt{\frac{\sum_i f_i \cdot L_i^2}{\sum_i f_i} - \mu^2} = \sqrt{\frac{\sum_i OD_i \cdot L_i}{\sum_i \frac{OD_i}{L_i}} - \mu^2}$$

where *ODi* is the chemiluminescent signal and *Li* is the length of the TRF at position *i* (16). The calculation takes into account the higher signal intensity from the larger TRFs because of multiple hybridization of the telomere-specific hybridization probe. Thus the frequency *fi* of the telomeres of length *Li* is proportional to the ratio *ODi/Li*, for all *i*.

Results

BrdU Selection and Telomere Length Analysis

Cultures of NF and HCA2 (MJ90) cells used in these studies reach senescence at about 55 and 70 PDs in culture, respectively. For BrdU selection and telomere length analysis, NF cells were used in PD 25 and nearly senescent PD 45 cultures. We used the classic method of BrdU selection (14,15), because BrdU is a nucleotide analog that incorporates into the DNA of all cycling cells. This incorporation is toxic to proliferating cells after long treatment times in combination with the addition of 33258 Hoechst dye and exposure to cool white fluorescent light. Using this approach, we were able to remove all cycling cells from the culture in 4–5 weeks of treatment. Noncycling cells remained viable, demonstrating a typical senescent phenotype and absence of any visible damage from the exposure to BrdU, Hoechst dye, and light (Figure 2). Total genomic DNA was isolated from the BrdU-selected fraction of senescent cells as well as from untreated cultures, digested with RsaI and HinfI restriction enzymes, and used for Southern blot analysis (Figure 3A). After densitometry (Figure 3B and C), we determined telomere length distribution, mean telomere lengths, and standard deviation for all samples as described in Experimental Procedures. For cells selected at PD 25, the measured value for mean TRF length (μ) was 5.48 kb, and that for standard deviation was 1.98; these values were similar to values measured for untreated cultures (5.81 kb and 2.13, respectively) (Figure 3B). Similarly, for cells selected at PD 45, the measured value for mean TRF length (μ) was 4.19 kb, and that for standard deviation was 2.04; again, these values were similar to those measured for untreated culture (4.08 kb and

→

Figure 3. Telomere length analysis of untreated and bromodeoxyuridine (BrdU)-selected fibroblast cultures at 25 (young) and 45 (senescent) population doublings (PDs). **A,** Southern blot analysis of untreated cultures (U) and BrdU-selected (B) fractions. Mw = molecular weight marker in kilobases. **B,** Optical density (OD) distributions and relative frequency distributions of telomere lengths of both untreated (red) and BrdU selected (blue) cells at PD 25. Mean telomere lengths (μ) of untreated culture is 0.33 kb greater than that of BrdU-selected fraction. **C,** Optical density distributions of telomere lengths of both untreated (red) and BrdU-selected (blue) cells at PD 45. Mean telomere lengths (μ) of untreated culture is 0.11 kb shorter than that of BrdU-selected fraction.

A

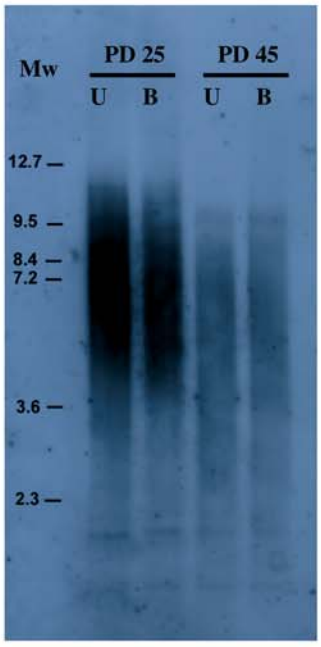

B

PD 25

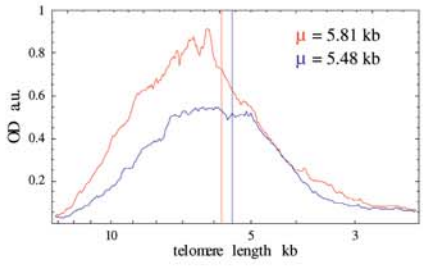

Optical density distribution

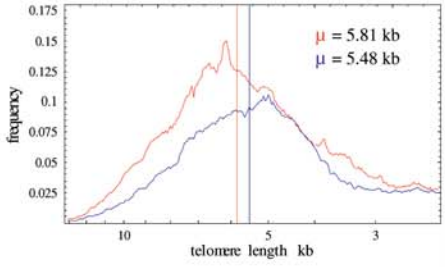

Frequency distribution

(——) = untreated culture at PD 25; (——) = BrdU selected fraction at PD 25

C

PD 45

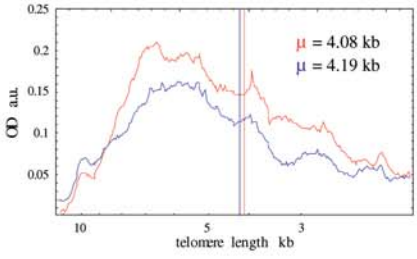

Optical density distribution

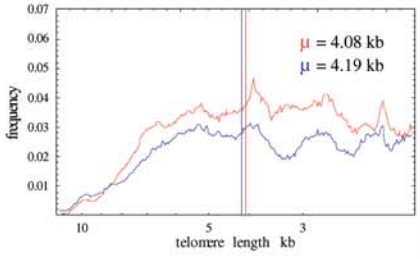

Frequency distribution

(——) = untreated culture at PD 45; (——) = BrdU selected fraction at PD 45

Table 1. Summarized Results of Telomere Length Analysis of Dividing (Young) and Nondividing (Senescent) NF and HCA2 Fibroblast Fractions Isolated Upon DiI Labeling and Flow Cytometry Separation at PD 19, and Telomere Length Analysis of Untreated and BrdU-Selected NF Fibroblast Cultures at 25 (Young) and 45 (Presenescent) PDs

			BrdU Selection			
	DiI Separation, PD 19		PD25		PD45	
Cell Type	"Young" Fraction	"Senescent" Fraction	Total Culture	Selected Cells	Total Culture	Selected Cells
NF	6.37	6.34	5.81	5.48	4.08	4.19
HCA2	7.56	7.49	—	—	—	—

Note: All values represent mean telomere lengths in kilobases.

NF = normal human foreskin fibroblast; DiI = 1,1′-dioctadecyl-3,3,3′,3′-tetramethylindocarbocyanineperchlorate; PD = population doubling; BrdU = bromodeoxyuridine.

1.92, respectively) (Figure 3C). These results demonstrate that telomeres of BrdU-selected, early-senescing cells shorten at the same rate as do their cycling counterparts (see Table 1).

A major drawback of this method is that it involves comparison of telomere lengths of the fraction of senescent cells with those of the entire, heterogeneous, untreated culture. Therefore, we decided to label cells with DiI and then separate cycling and noncycling cells from the same culture to perform a comparative analysis of their telomere lengths.

Cell Sorting and Telomere Length Analysis

NF or HCA2 cells were stained with DiI (17) at PD 19, cultured for 5–7 days, and submitted to flow cytometric analysis, as described in Experimental Procedures. This dye integrates into cell membranes and fluoresces orange-red (Figure 4). It has absorption and fluorescence emission maxima separated by about 65 nm, facilitating fluorescent detection efficiency. DiI labeling does not appreciably affect cell viability or basic physiological properties (17). Labeled fibroblasts used in these experiments did not demonstrate any visible changes in growth rate, morphology, or viability when compared with untreated controls (data not shown). As labeled cells divide, each daughter cell inherits approximately 50% of the dye, in the next generation 25%, and so on. Flow cytometric analysis of the labeling intensities of cultured cells allowed for determination of the number of cell division cycles through which individual cells had progressed. Fluorescence signals detected from successive generations of DiI-labeled cells were quite broad, and overlapped to some extent (Figure 1B, gray field). However, it was possible to distinguish cells that had undergone 5–6 divisions from nondividing cells (Figure 1D). Cells were cultured for 5–7 days prior to flow cytometric analysis and sorting (Figure 1C). Positive control cells were cultured for the same period of time and then stained on the day of sorting. Negative controls were unstained cells cultured for 5–7 days (Figure 1B).

A sample from both cycling and noncycling fractions was further cultured to examine morphology and frequency of SA-β-gal staining (Figure 1C), a reliable marker for the senescent phenotype (5). The subpopulation of cycling cells (blue fraction in Figure 1C) demonstrated a characteristic young morphology and very low frequency of SA-β-gal staining, typically less than 5%. In contrast, the noncycling subpopulation of cells (red fraction in Figure 1C) demonstrated a typical senescent morphology and high frequency and intensity of SA-β-gal staining, typically more than 97%.

Immediately following cell sorting, total genomic DNA was isolated from both fractions for telomere repeat length analysis as described above (Figure 5A). Densitometry (Figure 5B) and calculation of telomere lengths distributions, mean telomere length, and standard deviation were calculated as above. Cycling cells had a mean telomere length of 6.378 kb and standard deviation of 2.247, which were the same as those of the senescent fraction (6.347 kb and 2.163, respectively) (Figure 5B).

Similar results were obtained with normal human neonatal foreskin fibroblast cells, HCA2 (MJ90) (Table 1). These results were also the same as those obtained from the BrdU experiment, demonstrating that telomeres of

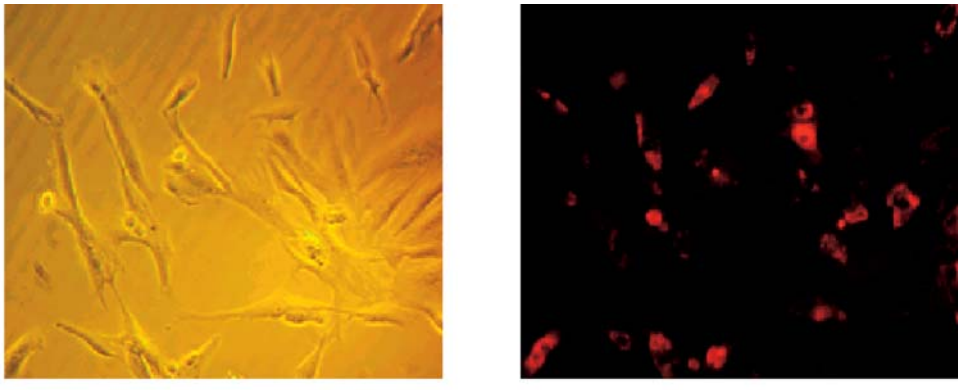

Figure 4. DiI (1,1′-dioctadecyl-3,3,3′,3′-tetramethylindocarbocyanineperchlorateI) labeling of cells before growth and flow cytometry. DiI stained outer and inner cell membranes. **A,** Cells under phase contrast; **B,** same cells under ultraviolet light.

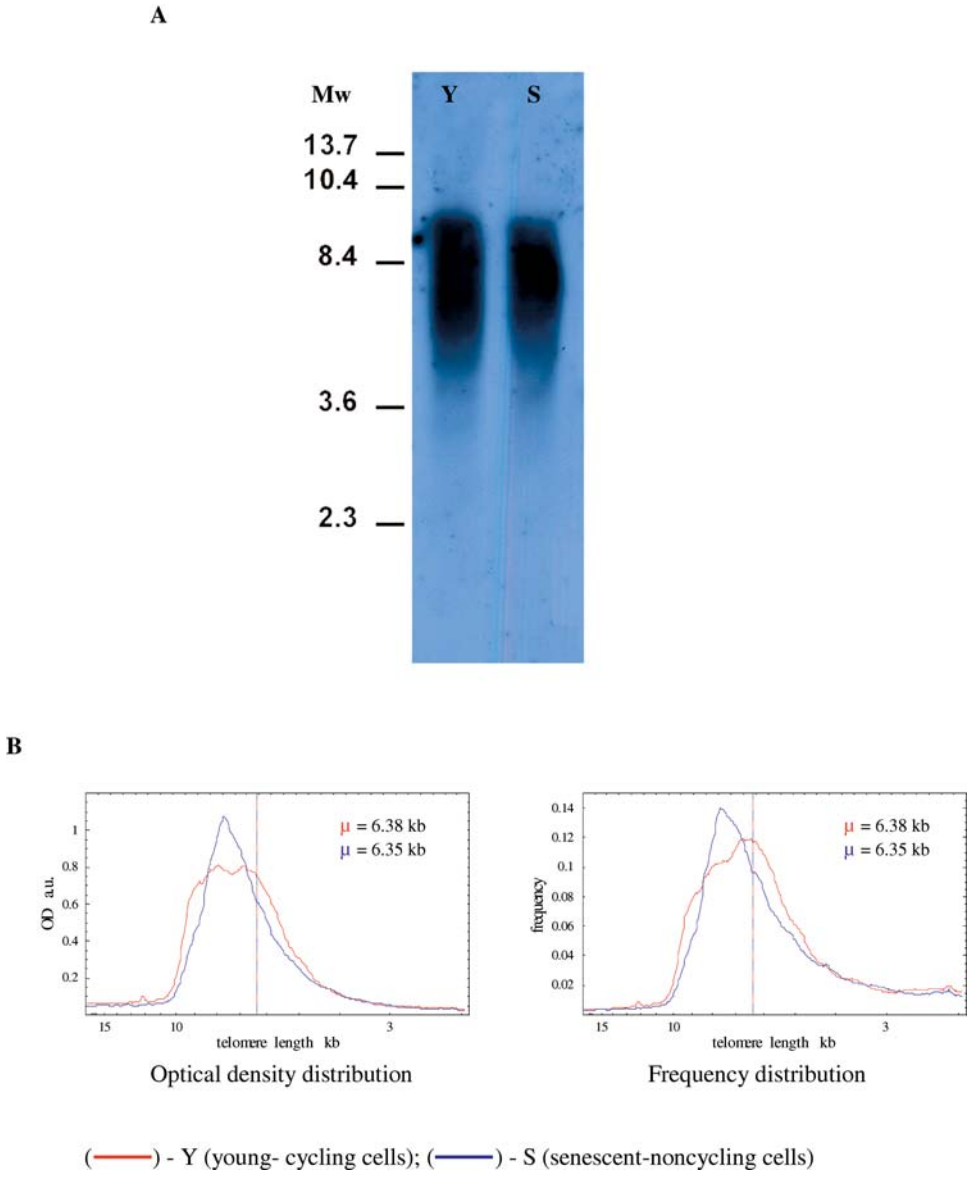

Figure 5. Telomere length analysis of dividing (young) and nondividing (senescent) fibroblast fractions isolated upon 1,1′-dioctadecyl-3,3,3′,3′-tetramethylindocarbocyanineperchlorate (DiI) labeling and flow cytometry separation at population doubling (PD) 19. **A,** Southern blot analysis of dividing (Y) and nondividing (S) cells. Mw = molecular weight marker in kilobases. **B,** Optical density distributions and relative frequency distributions of telomere lengths of both dividing (red) and nondividing (blue) cells. Mean telomere lengths (μ) of both fractions of cells are practically the same, differing by only 0.03 kb.

early-senescing cells shorten at the same rate as their cycling counterparts.

Discussion

The appearance of individual senescent cells in normal cell cultures (described as Sudden Senescence Syndrome [SSS]) (8,10) has led to the development of a few models attempting to explain this phenomenon. The stochastic appearance of senescent cells was first demonstrated by the experiments of Smith and Whitney (8), in which the division potential of the two daughter cells from a single mitotic division was determined. It was found that the doubling potential between two cells arising from a single mitotic event could vary from 0 to more than 8 PDs. Thus, cells can potentially senesce within one cell division, long before the terminal, nondividing phase of the culture as a whole. This phenomenon is continuously present in proliferating cultures, as was demonstrated by consecutive subcloning experiments (8). These results indicated that individual subclones of the same culture constantly generate heterogeneity in proliferative potential of the individual cells, resulting in a distinct bimodal distribution of cells. This heterogeneity is an intrinsic property of the culture so that a single clone produces a new bimodal distribution when it is subcloned again (8). The frequency of SSS increases almost exponentially as the culture approaches its maximum

number of divisions (8,10). It is interesting that a similar heterogeneity in proliferative potential of the individual cells in immortal human cell populations has been observed, as well as that heterogeneity is rapidly generated following subcloning (18,19).

In the last few years, data have implicated the dynamics of telomere shortening in the stochastic aspect of loss of proliferation in individual cells during cellular aging. Proposed models include stochastic changes in the levels or affinities of proteins that cap and uncap telomeres as they shorten (11), accelerated telomere shortening in a subpopulation of cells caused by stress via telomere-independent mechanisms (12,13), or abrupt shortening of a single telomere (10). Because there are indications that gradual telomere shortening cannot explain the rapid development of intraclonal variation or the large differences in doubling potentials between the products of a single mitotic event, we previously proposed a molecular model that could explain SSS (10). This model is based on both gradual and abrupt telomere shortening in which the main contributor to telomere erosion is progressive loss of terminal repeats superimposed on occasional catastrophic telomere deletion as a result of intrachromatid recombination. The latter event is initiated by strand invasion of the 3′ overhang into the telomeric and subtelomeric border region followed by formation of a t-loop; this structure has been demonstrated to be present in normal and immortal human and mouse cells (20). Our model explains the gradual increase of senescent cells in the culture by proposing that long telomeres have a stable conformation and a low probability of undergoing abrupt shortening but, as telomere shortening progresses, the probability of conformation changes to an unstable form increases almost exponentially (Figure 6). It is difficult to explain the daughter cell experiment (8) by stochastic uncapping of telomeres, because a sister cell would not be able to continue to divide for many more PDs as has been described (8). Additionally, although the senescent phenotype can be induced by a variety of stresses that are telomere-independent and inhibit cell growth [i.e., generalized DNA damage (21), oncogene activation (22), or changes in histone acetylation by inhibition of histone deacetylases {HDACs} (23)], it is difficult to visualize that the accelerated telomere shortening of all the telomeres in one sister cell could cause loss of proliferation in that cell, while the other sister cell continues to divide.

Our present results demonstrating that the mean telomere length is essentially the same in both cycling (young) and noncycling (senescent) fractions of cells separated from the same, heterogeneous, mass culture strongly support the idea that, under normal cell culture conditions, abrupt telomere shortening of one or very few chromosomes is the most probable mechanism that determines the generation of heterogeneity in cell populations. This idea is consistent with studies in which the length of individual Xp/Yp allele telomere length was determined and found to vary greatly in clones from a mass culture (24). These results are also in agreement with our recent findings with human telomerase reverse transcriptase (hTERT)-immortalized fibroblast mass cultures, in which large cells with a senescent phenotype were separated from small, young cells (25). There was no detectable difference in telomere length between the two populations. These data were further confirmed by labeling telomeres with a fluorescent probe followed by cell sorting. One of the cell lines analyzed was HCA2 (MJ90) cells used in this study, as well as IMR90 and LF1 cells (human fetal lung fibroblast cultures).

Recently, Martin-Ruiz and colleagues (13) performed flow cytometric analysis, including lipofuschin fluorescence (this increases as cells become senescent), to separate young and senescent cells from cultures of MRC5, human fetal lung fibroblasts. They found that in these cells the maximum telomere length remained the same at all PDs examined as well as in sorted senescent cells. However, average telomere length was decreased in the senescent populations. Real-time PCR was performed to further validate this measure of average telomere length. Their hypothesis is that stress-induced cell-to-cell variation of accelerated telomere shortening is the main cause of the intrinsic heterogeneity in the division potential of human fibroblasts. One possible explanation for the difference in our results could be that MRC5 cells, in contrast to the skin fibroblast cells used in our studies, require more of these events to occur before entering senescence; therefore, early-senescent cells in those cultures have shorter average telomeres.

We also used BrdU incorporation to selectively kill off cycling cells. Michishita and colleagues (26) have reported the induction of a senescent-like phenotype in HeLa cells following exposure to BrdU. However, they used high concentrations of BrdU (50 μM), and studied only the immortal cell line HeLa. Loss of cell proliferation was observed within 3–5 days of exposure, and all the cells became senescent-like with no cell death observed. We used the classical approach of treatment with 20 μM BrdU, followed by Hoechst dye and/or light exposure to selectively kill off proliferating cells; this required 3–4 weeks of repeated treatment (14,15). By initiating such treatments with even early PD cultures, one can select for the senescent cells present because the percentage of low doubling potential cells has been demonstrated to be as high as 30% in a culture at PD 3 (27,28). We also know that HCA2 (MJ90) cells do not increase p16 levels at senescence (unpublished observations) similar to BJ (HCA3 cells), thus the BrdU treatment did not cause ''stasis.'' Furthermore, we obtained the same results with both BrdU selection and DiI sorting.

Because our studies have shown that the mean telomere length is essentially the same in both cycling (young) and noncycling (senescent) fractions of cells separated from the same culture, we cannot rule out uncapping of a single telomere as a mechanism that results in division cessation. The identification of circular telomeric DNA in some mammalian cell lines (29), the presence of ultrashort, single telomeres in senescent human cells (24), generation of t-loop-sized deletions at human telomeres by homologous recombination (30), along with the observations of Hemann and colleagues (31) and Smith and Whitney (8) favor our model of catastrophic telomere deletion (Figure 6) as the mechanism that induces the stochastic p21/pRB-mediated permanent cell-cycle arrest observed in normal and immortal human cell cultures.

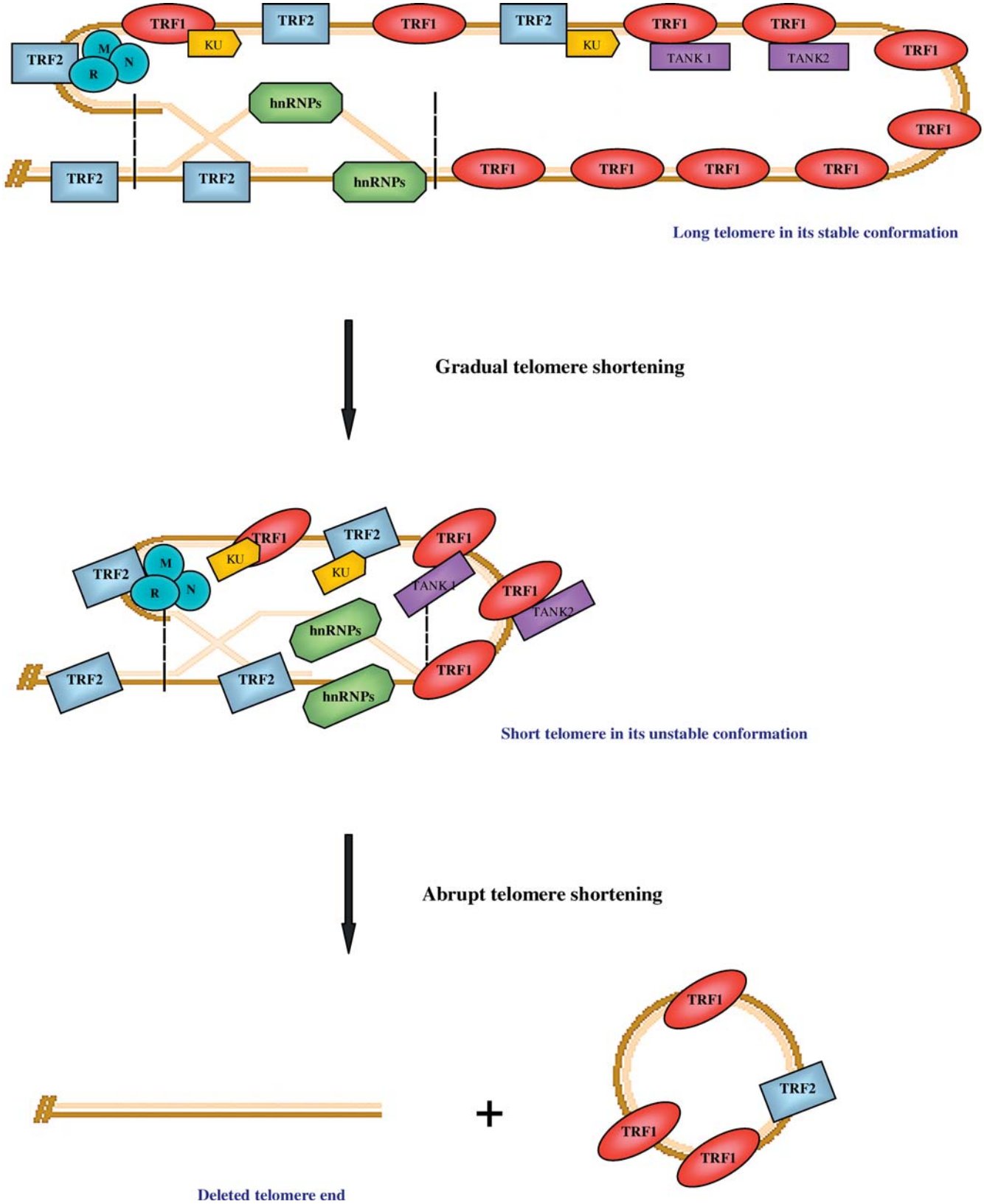

Figure 6. T-loop formation is stabilized by specific telomere-binding proteins. Model is based on a combination of both gradual and abrupt telomere shortening. Gradual telomere shortening occurs as a consequence of the inability of DNA polymerase to replicate the very end of chromosomal DNA as well as exonuclease degradation of the 5′ strand at telomere ends. When a telomere reaches its critical length, it switches from stable to unstable conformation, which can provoke Holiday structure formation and a subsequent recombination event. Abrupt telomere shortening is predicted to occur through telomere 3′-single-strand self-invasion at or near the telomere/subtelomere border region (between vertical dotted lines). Recombination results in a deletion of distal repeats through circularization.

ACKNOWLEDGMENTS

This work was supported by Croatian Ministry of Science, Education and Sports Grants 0098077 (to M.F. and I.R.) and 0037115 (to M.H.), and by the Ellison Medical Foundation (to O.M.P.-S.).

Address correspondence to Ivica Rubelj, PhD, Department of Molecular Biology, Ruđer Bošković Institute, Bijenička 54, Zagreb 10000, Croatia. E-mail: rubelj@rudjer.irb.hr

REFERENCES

1. Hayflick L, Moorhed PS. The serial cultivation of human diploid cell strains. *Exp Cell Res.* 1961;25:585–621.
2. Hayflick L. The limited in vitro lifetime of human diploid cell strains. *Exp Cell Res.* 1965;37:614–636.
3. Matsumura T, Zerrudo Z, Hayflick L. Senescent human diploid cells in culture: survival, DNA synthesis and morphology. *J Gerontol.* 1979;34:328–334.
4. Norwood TH, Smith JR, Stein GH. In: *Handbook of the Biology of Aging*, Schneider EL, Rowe JW, eds. San Diego, CA: Academic Press; 1990;131–154.
5. Dimri GP, Lee X, Basile G, et al. A biomarker that identifies senescent human cells in culture and in aging skin in vivo. *Proc Natl Acad Sci U S A.* 1995;92:9363–9367.
6. Shelton DN, Chang E, Whittier PS, Choi D, Funk WD. Microarray analysis of replicative senescence. *Curr Biol.* 1999;9:939–945.
7. Funk WD, Wang CK, Shelton DN, Harley CB, Pagon GD, Hoeffler WK. Telomerase expression restores dermal integrity to in vitro-aged fibroblasts in a reconstituted skin model. *Exp Cell Res.* 2000;258: 270–278.
8. Smith JR, Whitney RG. Intraclonal variation in proliferative potential of human diploid fibroblasts: stochastic mechanism for cellular aging. *Science.* 1980;207:82–84.
9. Rubelj I, Huzak M, Brdar B. Sudden senescence syndrome plays a major role in cell culture proliferation. *Mech Ageing Dev.* 2000; 112:233–241.
10. Rubelj I, Vondraček Z. Stochastic mechanism of cellular aging–Abrupt telomere shortening as a model for stochastic nature of cellular aging. *J Theor Biol.* 1999;197:425–438.
11. Blackburn EH. Telomere states and cell fates. *Nature.* 2000;408:53–56.
12. von Zglinicki T. Oxidative stress shortens telomeres. *Trends Biochem Sci.* 2002;27:339–344.
13. Martin-Ruiz C, Saretzki G, Petrie J, et al. Stochastic variation in telomere shortening rate causes heterogeneity of human fibroblast replicative lifespan. *J Biol Chem.* 2004;279:17826–17833.
14. Burmer GC, Norwood TH. Selective elimination of proliferating cells in human diploid cell cultures by treatment with BrdU, 33258 Hoechst and viible light. *Mech Ageing Dev.* 1980;12:151–159.
15. Gorman SD, Cristofalo VJ. Reinitiation of cellular DNA synthesis in BrdU-selected nondividing senescent WI-38 cells by simian virus 40 infection. *J Cell Physiol.* 1985;125:122–126.
16. Harley CB, Futcher AB, Greider CW. Telomeres shorten during ageing of human fibroblasts. *Nature.* 1990;345:458–460.
17. Ledley FD, Soriano HE, O'Malley BW Jr, Lewis D, Darlington GJ, Finegold M. DiI as a marker for cellular transplantation into solid organs. *Biotechniques.* 1992;13:580, 582, 584–587.
18. Martinez AO, Norwood TH, Prothero JW, Martin GM. Evidence for clonal attenuation of growth potential in HeLa cells. *In Vitro.* 1978; 14:996–1002.
19. Pereira-Smith OM, Smith JR. Expression of SV40 T antigen in finite life-span hybrids of normal and SV40-transformed fibroblasts. *Somatic Cell Genet.* 1981;7:411–421.
20. Griffith JD, Comeau L, Rosenfield S, et al. Mammalian telomeres end in a large duplex loop. *Cell.* 1999;97:503–514.
21. Chen QM, Prowse KR, Tu VC, Purdom S, Linskens MHK. Uncoupling the senescent phenotype from telomere shortening in hydrogen peroxide-treated fibroblasts. *Exp Cell Res.* 2001;265:294–303.
22. Itahana K, Dimri G, Campisi J. Regulation of cellular senescence by p53. *Eur J Biochem.* 2001;268:2784–2791.
23. Tominaga K, Leung JK, Rookard P, Echigo J, Smith JR, Pereira-Smith OM. MRGX is a novel transcriptional regulator that exhibits activation or repression of the B-myb promoter in a cell type-dependent manner. *J Biol Chem.* 2003;278:49618–49624.
24. Baird D, Rowson J, Wynford-Thomas D, Kipling D. Extensive allelic variation and ultrashort telomeres in senescent human cells. *Nat Genet.* 2003;33:203–207.
25. Gorbunova V, Seluanov A, Pereira-Smith OM. Evidence that high telomerase activity may induce a senescent-like growth arrest in human fibroblasts. *J Biol Chem.* 2003;278:7692–7698.
26. Michishita E, Matsumura N, Kurahashi T, Suzuki T, Ogino H, Fujii M, Ayusawa D. 5-Halogenated thymidine analogues induce a senescence-like phenomenon in HeLa cells. *Biosci Biotechnol Biochem.* 2002;66: 877–879.
27. Smith JR, Hayflick L. Variation in the life-span of clones derived from human diploid cell strains. *J Cell Biol.* 1974;62:48–53.
28. Pereira-Smith OM, Smith JR. The phenotype of low proliferative potential is dominant in hybrids of normal human fibroblasts. *Som Cell Genet.* 1982;8:731–742.
29. Regev A, Cohen S, Cohen E, Bar-Am I, Lavi S. Telomeric repeats on small polydisperse circular DNA (spcDNA) and genomic instability. *Oncogene.* 1998;17:3455–3461.
30. Wang RC, Smogorzewska A, de Lange T. Homologous recombination generates t-loop-sized deletions at human telomeres. *Cell.* 2004;119: 355–368.
31. Hemann MT, Strong MA, Hao LY, Greider CW. The shortest telomere, not average telomere length, is critical for cell viability and chromosome stability. *Cell.* 2001;107:67–77.

Received October 19, 2004
Accepted January 12, 2005
Decision Editor: James R. Smith, PhD